Studies of the Mechanism of Electron-Ion Recombination. I

MANFRED A. BIONDI*
Westinghouse Research Laboratories, Pittsburgh, Pennsylvania
(Received 29 August 1962)

Microwave and optical techniques are used to study the loss of electrons during the afterglow following microwave discharges in noble gases, principally in neon and argon. The time and pressure dependences of the electron density decays follow a two-body volume electron-ion recombination law over a wide range of variables, yielding recombination coefficients in the range 10^{-7}–10^{-6} cc/sec for neon and for argon. The afterglow radiation is shown to originate in the volume of the ionized gas, far from the walls, and to decrease in intensity when the electron energy is momentarily increased. Both of these observations are consistent with volume recombination loss of electrons leading to the formation of excited atoms. Further, the intensity of the afterglow radiation is observed to vary in time in the same manner as the square of the electron density, and absolute intensity determinations in neon and in argon yield recombination coefficients consistent with the values obtained from the electron-density decay curves. As a test of the hypothesis that dissociative recombination, $X_2^+ + e \rightarrow X^* + X$, is responsible for the large recombination loss observed in microwave afterglows, measurements are made under conditions first where only Ar^+ ions and then where only Ar_2^+ ions are expected in the afterglow. The usual large recombination loss of electrons is observed when Ar_2^+ ions are present, but at the same charge densities, only ambipolar diffusion loss of electrons and Ar^+ ions is observed.

I. INTRODUCTION

THE recombination of free electrons with positive ions has been the subject of numerous theoretical and experimental investigations.[1,2] The recombination process which has been most extensively and successfully treated theoretically[3] is that involving the radiative capture of an electron by a positive ion, i.e.,

$$X^+ + e \rightarrow X^* + h\nu, \qquad (1)$$

where the superscripts + and * refer to ionized and excited states of the atom (or molecule), respectively. For thermal (~300°K) electrons, the recombination coefficient α (defined by the relation $dn_e/dt = -\alpha n_e n_+$, where n_e and n_+ are the electron and positive ion densities, respectively) was calculated to have values in the range 10^{-11}–10^{-12} cc/sec for various positive ions.[1]

Recent studies by Craggs and Hopwood[4] of the recombination of electrons and positive ions (H^+) in intensely ionized spark channels have yielded a spectral distribution of the radiation emitted and a magnitude of α appropriate to radiative recombination. However, much earlier Langmuir probe and spectroscopic studies by Kenty[5] (1928) and by Mohler and Boeckner[6] (1929) concerning recombination in afterglows of argon, cesium, and mercury discharges gave values which were some hundred times larger than radiative theory. The difficulties of the experiments were sufficiently great that these discrepancies between theory and experiment were attributed to defects in the measuring techniques.

The development of microwave techniques for obtaining accurate measurements of the average electron densities in ionized gases led to the discovery of recombination losses of electrons in afterglows of noble gas discharges[7] (e.g., neon and argon) which were more than 10^4 times the theoretical values for radiative recombination. In these studies, the experimental uncertainties were far too small to explain the discrepancy.

Earlier investigations of the night-time decay of electron density in the E layer of the ionosphere had led to the deduction of an effective recombination coefficient for the electrons of 10^{-8}–10^{-7} cc/sec.[8] After abandoning attempts to explain this loss in terms of *negative ion–positive ion* recombination, a new process, dissociative recombination between electrons and positive ions, was suggested to explain the large coefficient.[8] This process is illustrated schematically in Fig. 1. One has, initially, a *molecular* positive ion and an electron (state A). If the repulsive curve (B-C) of an excited state of the molecule crosses the ion curve at the appropriate point, the system may transfer to this state and begin to dissociate. Once the internuclear separation has increased slightly, the system can no longer revert to its original state by auto-ionization and the electron is trapped as the

* University of Pittsburgh and Westinghouse Research Laboratories, Pittsburgh, Pennsylvania.

[1] H. S. W. Massey, and H. S. Burhop, *Electronic and Ionic Impact Phenomena* (Oxford University Press, New York, 1952), Chaps. VI and X.

[2] L. B. Loeb, *Basic Processes of Gaseous Electronics* (University of California Press, Berkeley and Los Angeles, 1955), Chap. VI.

[3] Recently, three-body recombination involving two electrons and a positive ion has been successfully treated theoretically [see, for example, N. D'Angelo, Phys. Rev. **121**, 505 (1961), D. R. Bates and A. E. Kingston, Nature **189**, 652 (1961), R. W. P. McWhirter, *ibid.* **190**, 902 (1961), and E. Hinnov and J. Hirschberg, Phys. Rev. **125**, 795 (1962)]. However, this process is expected to be of importance only at rather high electron and ion densities ($n_{e,i} > 10^{12}$ cm^{-3}).

[4] J. D. Craggs, and W. Hopwood, Proc. Phys. Soc. (London) **59**, 771 (1947).

[5] C. Kenty, Phys. Rev. **32**, 624 (1928).

[6] F. L. Mohler and C. Boeckner, Bur. Standards J. Research **2**, 489 (1929).

[7] M. A. Biondi, and S. C. Brown, Phys. Rev. **76**, 1697 (1949).

[8] See, for example, D. R. Bates and H. S. W. Massey, Proc. Roy. Soc. (London) **A187**, 261 (1946) and H. S. W. Massey, in *Advances in Physics*, edited by N. F. Mott (Taylor and Francis, Ltd., London, 1952), Vol. I.

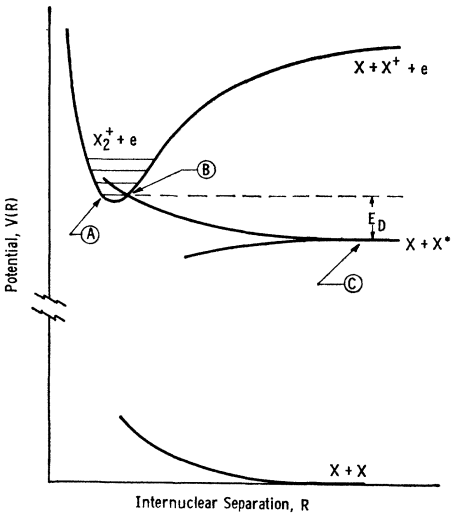

FIG. 1. Schematic representation of the dissociative recombination process, $X_2^+ + e \rightarrow (X_2^*)_{\text{unstable}} \rightarrow X^* + X + \text{kinetic energy}$.

molecule continues to dissociate (state C). In reaction form, this process may be written as

$$X_2^+ + e \rightarrow (X_2^*)_{\text{unstable}} \rightarrow X^* + X + \text{kinetic energy}. \quad (2)$$

Although no quantitative theory for this process was available, the radiationless capture of the electron was believed to be considerably more efficient than radiative recombination, and hence it was suggested that dissociative recombination was the origin of the large electron loss rate in the E layer.

Shortly after the publication of the microwave studies of recombination in helium, Bates[9] suggested that since molecular positive ions of the noble gases were known to exist, the large recombination coefficient found in helium was the result of the dissociative process. The present paper presents the results of a series of experiments designed (a) to determine the validity of the conclusion that electron-ion recombination is an important process in the microwave afterglow studies and (b) to determine the nature of the recombination process.

II. EXPERIMENTAL TECHNIQUES

Most of the experimental techniques used in these studies have been described in detail elsewhere; therefore, only a brief review of the methods will be given here. Microwave techniques are used to determine the average electron density during the afterglow following a pulsed discharge.[10] A simplified diagram of the apparatus is shown in Fig. 2. A gas sample of high purity[11] is admitted to the cylindrical quartz bottle inside a microwave cavity (resonant at ~3000 Mc/sec) by means of an ultra-high vacuum gas handling system.[12] A discharge, whose duration can be varied from 10 μsec to >1 msec, is initiated in the gas by power from the pulsed magnetron at the right. Under proper experimental conditions, the chief effect of the free electrons in the ionized gas is to change the resonant frequency of the cavity as a result of their dielectric effect. If the spatial distribution of the electrons in the bottle is known, absolute values of the average electron density can be obtained from the measured frequency shifts.

During the afterglow following the discharge, the changing electron density is determined by observing with a directional coupler the reflection from the cavity of a low power continuous signal from the klystron. When the changing electron density brings the resonant frequency of the cavity-plus-electrons into coincidence with the signal frequency, a minimum in reflected signal occurs. By noting the times at which minimum reflections occur for several different signal frequencies, the variation of frequency shift and, hence, of the electron density during the afterglow can be determined.

In addition to electron-density measurements, it is possible to determine the optical radiation emitted during the afterglow by means of an observing port in the side of the cavity. In some cases, the spectral distribution of the emitted radiation is determined by means of the spectrometer and photomultiplier (shown in the figure); in others the emission in broad wavelength regions is observed by means of glass absorption filters and a phtomultiplier which views the cavity directly. The photomultipliers are operated in two ways; in one, the photomultipliers are made continuously sensitive and their signals amplified and displayed on the oscilloscope. In the other, the photomultipliers are gated (made sensitive to radiation) for a fixed interval whose start can be delayed by various amounts with respect to the discharge. The output signals are fed to integrating circuits and electrometers. By averaging the signal over many afterglow cycles, the signal-to-noise ratio is

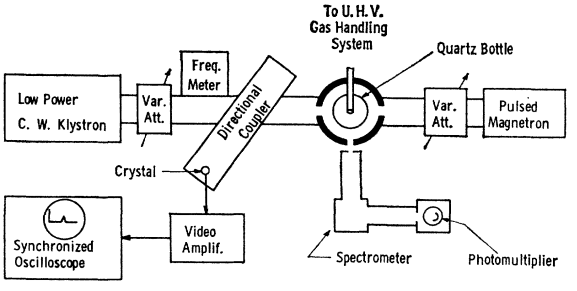

FIG. 2. Simplified block diagram of the microwave and optical apparatus used in the afterglow studies.

[9] D. R. Bates, Phys. Rev. **77**, 718 (1950); **78**, 492 (1950).
[10] M. A. Biondi, Rev. Sci. Instr. **22**, 500 (1951).
[11] The neon and argon gases used in these studies were reagent grade samples obtained from the Air Reduction Company. The helium gas was purified using liquid helium techniques; see M. A. Biondi, Rev. Sci. Instr. **22**, 535 (1951).
[12] See, for example, D. Alpert, J. Appl. Phys. **24**, 860 (1953).

greatly improved and thus very low levels of emitted radiation can be measured.[13]

III. RECOMBINATION AND DIFFUSION

The variation of electron density during the afterglow is, in general, the result of a number of competing processes. Let us consider a very simple model in which the initially ionized gas (plasma) contains only neutral atoms, electrons, and positive ions of one type. In addition, let the only significant electron removal processes be volume electron-ion recombination and ambipolar diffusion to the walls, where it is assumed that the charged particles are neutralized. Then, from continuity considerations, we find that

$$\partial n_e/\partial t = -\alpha n_e n_+ + D_a \nabla^2 n_e, \tag{3}$$

where n_e and n_+ are the electron and ion densities, respectively, and D_a is the ambipolar diffusion coefficient. Since the plasma must at all times be very nearly electrically neutral to avoid buildup of large electric fields, we have $n_e \simeq n_+$, so that the first term on the right may be replaced by $(-\alpha n_e^2)$. Numerical solutions of this general equation for particular geometrical configurations have been obtained by Oskam[14] and by Gray and Kerr[15]; we shall refer in more detail to their results later in the paper. For the present, let us consider three solutions to this equation:

(a) Recombination alone;

$$1/n_e = [1/n_e(0)] + \alpha t. \tag{4}$$

(b) Diffusion alone;

$$n_e = \sum_i a_i \exp(-t/T_i), \tag{5}$$

where $T_i = \Lambda_i^2/D_a$, Λ_i being the diffusion length for the ith spatial distribution mode.

(c) Fundamental (lowest diffusion mode plus small recombination.

In this case, we may approximate the last term of Eq. (3) by $(-n_e/T_1)$, obtained by using only the first term of the series solution of Eq. (5). The solution then becomes

$$n_e/(1+\alpha T_1 n_e) = n_e(0) \exp(-t/T_1)/[1+\alpha T_1 n_e(0)]. \tag{6}$$

Many of the electron decay curves obtained by various investigators[7,16,17] have been interpreted in terms of one of these three solutions, which are based on the aforementioned, simple model of the afterglow.

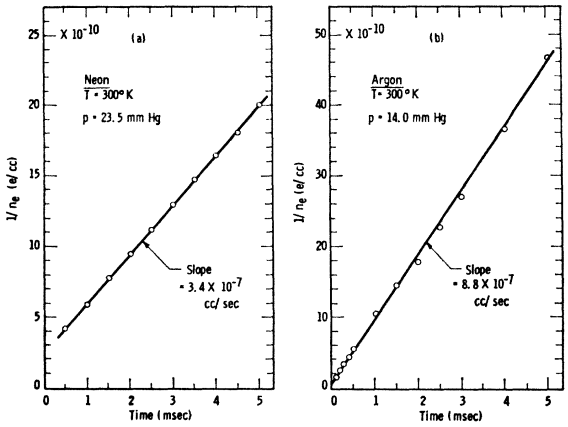

FIG. 3. Electron-density decay as a function of time in neon and in argon afterglows. The data are plotted as $1/n_e$ vs t to exhibit a recombination law dependence.

IV. STUDIES OF RECOMBINATION

A. Electron Density Measurements

The early microwave measurements were applied to the study of afterglows of helium.[18] At the time it was believed that, in view of the simplicity of the helium atom, the only significant afterglow process would be the ambipolar diffusion of He^+ ions and electrons. At low pressures ($\sim$1–5 mm Hg) and late times in the afterglow the time and pressure dependences of the electron decay were reasonably consistent with fundamental mode ambipolar diffusion loss. (Since the diffusion coefficient varies inversely with gas density, the decay times increase linearly with pressure.) However, when similar studies were carried out in neon,[7] the electron decay neither showed a pressure dependence nor did it fit the diffusion time dependence. The recombination solution, Eq. (4), was found to provide a much better fit to the data, although the coefficient ($\alpha \sim 10^{-7}$ cc/sec) was extremely large [see Fig. 3(a)]. A search for radiation accompanying the recombination process, using a crude photomultiplier arrangement, revealed an afterglow persisting for milliseconds after the termination of the discharge.

The two experimental results, that the data fit Eq. (4) over a range of electron density of approximately a factor of 10 and that persistent afterglow radiation was emitted, were taken as evidence that electron-ion recombination was a dominant electron removal process in neon. Similar results were obtained in argon[19] [see Fig. 3(b)]. Rather cursory recombination studies in helium, hydrogen, nitrogen, and oxygen[7] also indicated coefficients in the range 10^{-8}–10^{-6} cc/sec, although in many cases the fit of the data to Eq. (4) extended over

[13] The gated photomultiplier and time sampling techniques used were based on those developed by A. O. McCoubrey, Phys. Rev. **93**, 1249 (1954).

[14] H. J. Oskam, Philips Res. Repts. **13**, 335, 401 (1958).

[15] E. P. Gray and D. E. Kerr, in *Proceedings of the Fourth International Conference on Ionization Phenomena in Gases, Uppsala, Sweden* (North-Holland Publishing Company, Amsterdam, 1960), and Ann. Phys. (New York) **17**, 276 (1962).

[16] R. B. Holt, J. M. Richardson, B. Howland, and B. T. McClure, Phys. Rev. **77**, 239 (1950); R. A. Johnson, B. T. McClure, and R. B. Holt, *ibid.* **80**, 376 (1950).

[17] A. C. Faire and K. S. C. Champion, Phys. Rev. **113**, 1 (1959).

[18] M. A. Biondi and S. C. Brown, Phys. Rev. **75**, 1700 (1949).

[19] M. A. Biondi, Phys. Rev. **83**, 1078 (1951).

only a limited electron density range (a factor of 3) before departing in the direction of diffusion controlled loss. In particular, in helium the relatively large ambipolar diffusion coefficient and relatively small recombination coefficient compared to the other gases led to difficulties in obtaining an accurate value of α as a result of a very limited range over which Eq. (4) was obeyed (see Fig. 3 of reference 18). However, here again the observation of afterglow radiation lasting many milliseconds was taken as additional evidence for the existence of the recombination process.

During this period, a group at Harvard University had been independently studying recombination in afterglows, using precision spectroscopic techniques.[16] When they added microwave techniques to their measurements to permit absolute determinations of n_e, and thus of α, they also obtained large recombination coefficients and extended the measurements to other gases such as cesium, mercury, krypton, and xenon.

In many of the recombination studies, from the early microwave studies to the present, values of α have been deduced either from limited fits of Eq. (4) or from an analysis of the mixed diffusion and recombination cases, such as is illustrated by Eq. (6). Recently, Gray and Kerr[15] have developed quantitative criteria for estimating the errors to be expected from such analyses, although their treatment has been limited to special geometries (infinite parallel planes, the infinite cylinder, and the sphere). They show that, as one might intuitively expect, if the recombination rate is many times larger than the fundamental diffusion rate, reasonably accurate values of α can be obtained from electron decay data. Thus, the measurements in neon and argon are probably satisfactory,[20] On the other hand, the value of α in helium of $\sim 10^{-8}$ cc/sec deduced from electron-density decay should be seriously in error. One may conclude from their analysis, therefore, that deduction of α values from experimental data which fit Eq. (4) over a sufficient range of electron densities provides the most direct and unambiguous determination of electron-ion recombination rates.[21]

B. Afterglow Radiation Studies

1. Spatial Distribution

In view of the difficulty in explaining the very large recombination coefficients in terms of radiative recombination,[22] the suggestion was advanced that the decay of electrons was actually by diffusion to the walls and that the emitted afterglow radiation occurred as a result of wall recombination between positive ions and electrons. Although this suggestion is regarded as unlikely, since the pressure and the temporal dependences of diffusion loss are quite different from those of two-body volume recombination, and recombination at a wall should so perturb the atomic states that the characteristic line spectra should not be emitted, an experiment has been devised to observe the spatial points of origin of the afterglow radiation.

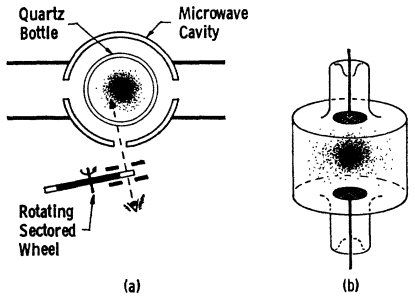

FIG. 4. Sketches of the visually observed spatial distribution of the afterglow radiation from (a) the microwave discharge and (b) a pulsed dc discharge.

A rotating wheel and slit system is used to provide a trigger to start the discharge and also to permit visual observation of the discharge tube. The phasing of the discharge is such that, for a period lasting from ~ 500 μsec before the start of the discharge to ~ 500 μsec after the discharge is terminated, the viewing path is blocked. Thus, only afterglow radiation can be observed when using this device. The microwave afterglow is viewed through a wide slit in the side of the TM_{010} mode cavity [see Fig. 4(a)]. By moving the sectored wheel, it is possible to view most of the quartz bottle. To a dark adapted eye, the afterglows of helium and neon are clearly visible as luminous spheres of decreasing intensity toward the quartz walls. As an added test, to avoid the limited viewing angle caused by the microwave cavity, a glass discharge tube with metal electodes has been attached to the same gas handling system [see Fig. 4(b)]. A dc pulse of the same duration as the microwave pulse (~ 500 μsec) is used to ionize the gas. In this case, the discharge tube can be viewed from

[20] For the curves of Fig. 3, it is estimated that the actual recombination values are approximately 20–30% less than the values obtained directly from the slopes of the curves. This estimate has been obtained by using Gray and Kerr's analysis, reference 15, for a spherical geometry and normalizing our cylindrical container to their curves by means of the fundamental diffusion length, Λ_1.

[21] It should be noted that, for extremely inhomogeneous excitation of the discharge, in which the maximum electron and ion densities occur near a bounding wall, it is possible to get an apparent recombination law decay which is the result of higher diffusion modes. See K. B. Persson and S. C. Brown, Phys. Rev. **100**, 729 (1955). Such asymmetrical charge distributions can be detected by monitoring the spatial distribution of the afterglow recombination radiation with a gated photomultiplier and were not observed in the present work.

[22] The theory given is reference 7, purporting to explain the large α's, is incorrect; if one calculates classically the radiation of an electron accelerated in the field of a positive ion, one must Fourier analyze the spectrum emitted and discard those frequencies which lead to the emission of photons of energy greater than the total energy difference between the electron in the free and bound states. This added condition leads to a large reduction in the calculated value of the recombination coefficient, bringing it into agreement with the results of quantum mechanical calculations of the radiative process. This effect was pointed out to the author by T. Holstein, private communication.

almost any angle. Once again, the afterglow radiation is clearly found to come from the volume of the gas, with maximum apparent intensity at the center of the vessel, decreasing toward the walls. This persistent afterglow radiation coming from the volume is difficult to explain in terms of processes other than volume electron-ion recombination.

2. *Effect of Electron Energy*

The rates of the various possible recombination processes (e.g., radiative recombination and dissociation recombination) are, in most cases, expected to decrease with increasing electron energy.[23] Thus, if one suddenly raises the electron energy during the afterglow, the recombination process may be slowed. Normally, care is taken to use a sufficiently low power microwave probing signal in making electron density measurements to avoid raising the electron energy above the gas temperature. However, if one increases the power level of the probing signal, then at the time the cavity resonant frequency comes into coincidence with the signal frequency the electron energy is raised and then falls back to thermal energy when the cavity no longer resonates at the signal frequency (and, therefore, most of the incident power is reflected).

If the afterglow radiation is the result of recombination, raising the electron energy may decrease the radiation intensity. On the other hand, if the afterglow radiation is the result of some excitation process involving electron impact, the intensity should increase since the electron energy is thermal prior to the absorption of microwave power. A photomultiplier sensitive to visible and near uv radiation has been used to view the emitted afterglow radiation. The results of studies of pure helium at 2.1 mm Hg pressure are shown in Fig. 5, which is a multiple exposure photograph of the oscilloscope traces. Curve B represents the observed afterglow intensity when no microwave probing signal is used (it has been displaced slightly vertically to prevent confusion with curve A, which is undisplaced). When the probing microwaves are turned on at an increased power level, the signal reflected from the cavity is as shown in the lower part of the figure. When the cavity is far off resonance, essentially all of the incident power is reflected. However, at resonance the cavity absorbs energy and the reflected signal decreases.[24] At the times of increased

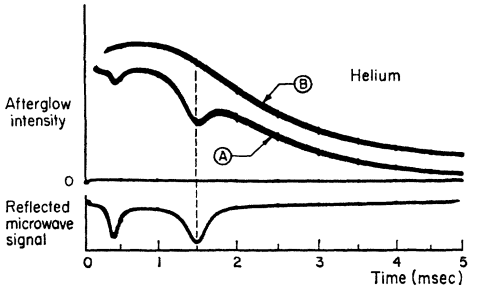

FIG. 5. Observed "quenching" of the afterglow radiation when the electron energy is raised above thermal equilibrium values by the microwave probing signal. The occurrence of quenching at two times in the afterglow is the result of the fact that the cavity absorbs energy when the electron density reaches a particular value. Since, in these afterglows, the electron density at first increases and then decreases as a result of metastable atom ionization (see reference 24) the critical density occurs at two distinct times.

electron energy[25] the afterglow radiation is observed to decrease (curve A). This phenomenon was independently observed by Goldstein, Anderson, and Clark[26] who named the effect "afterglow quenching" and developed semiquantitative techniques for using it in recombination studies.

A similar radiation "quenching" was observed in neon afterglows. In addition, it was possible to increase the probing signal power sufficiently far beyond the "quenching" level to give the electrons enough additional energy to excite ground-state neon atoms to radiating states, leading to an increase in afterglow intensity during resonance between cavity and signal.

3. *The Electron Density and the Emitted Intensity*

According to Eqs. (1) and (2), both radiative and dissociative recombination may lead to the formation of excited levels of the atom, which then emit their characteristic line spectra. Thus, if we neglect excitation and cascading processes, the formation and decay of the jth excited state is given by

$$dn_j/dt=\alpha_j n_e n_+ - R_j n_j, \tag{7}$$

where n_j is the density of the jth state, α_j is the recombination coefficient into the jth state, and R_j is the radiative decay frequency of this state. The intensity of a given line emanating from this state is proportional to the density of the atoms n_j times the emission frequency for this line, R_{jl}, where $R_j=\sum_l R_{jl}$, l being the index of lower states reached from state j in the radia-

[23] For the case of dissociative recombination, if the unstable excited molecule curves cross the molecular ion curve (point B of Fig. 1) above its minimum, the electron will require kinetic energy to reach the unstable molecule curve and therefore, the recombination coefficient will at first *increase* with increasing energy. However, at sufficiently high electron energies the recombination coefficient will again decrease as one increases the electron energy because the dissociation time relative to the autoionization time becomes longer as one moves up the unstable molecule curve further to the left of B.

[24] It will be seen that there are two times at which the cavity frequency equals the signal frequency. This is the result of the fact that, in the afterglow, the electron density at first *increases* and then decreases as a result of ionization produced by the collision of pairs of metastable helium atoms. This process has been studied in detail; however, to avoid undue complication we have not included it in our general considerations for this paper. See, M. A. Biondi, Phys. Rev. **82**, 453 (1951); **88**, 660 (1952).

[25] The slight delay between maximum power absorption and minimum light intensity is consistent with the calculated electron energy gain time in the microwave field.

[26] L. Goldstein, J. M. Anderson, and G. L. Clark, Phys. Rev. **90**, 486 (1953); and C. L. Chen, C. C. Leiby, and L. Goldstein, *ibid.* **121**, 1391 (1961).

tive transitions. Since $1/R_j$ is very short ($\lesssim 10^{-7}$ sec) compared to the measuring time scale for observing electron density decay, one has, at times large compared to $(1/R_j)$, $dn_j/dt \ll R_j n_j$ and $\alpha_j n_e e_+$; i.e.,

$$(\text{Int})_{jl} \sim R_{jl} n_j \simeq [(R_{jl}/R_j)\alpha_j] n_e n_+. \quad (8)$$

In cases where the recombination process is associated with the dominant positive ion type and negative ion formation is absent, $n_e \simeq n_+$, and one expects the recombination intensity to be proportional to n_e^2.

The results of total intensity and electron density measurements in the neon afterglow are shown in Fig. 6. The $(\text{intensity})^{1/2}$ curve is normalized in value to the electron density curve at 2.5 msec. This example of our data was chosen to illustrate the point that, under conditions where a single positive ion type is expected to predominate, even after the curves deviate from the recombination law as a result of diffusion effects, the proportionality between $(\text{Int})^{1/2}$ and n_e is maintained.

Similar results demonstrating the proportionality between $(\text{Int})^{1/2}$ and n_e have also been obtained in argon. Discussion of the helium afterglow radiation, which is complicated by the appearance of band spectra at higher pressures, is deferred to part II of this paper.

From Eq. (8) it will be seen that a determination of the absolute intensity of the emitted recombination radiation, coupled with a determination of the electron density at the same instant provides a measure of α_j. If one is able to detect a sufficient wavelength range of radiation so that the detected lines originate from a large number of the excited levels of the atom formed during recombination, then the total quantum yield gives an indication of the magnitude of α. Of course, this method fails to account for recombination directly to the ground state or to metastable states and therefore provides a lower bound on the actual value of α.

Total intensity measurements of the radiation emitted from afterglows of helium, neon, and argon were made using a calibrated photomultiplier (RCA Type 931 A).

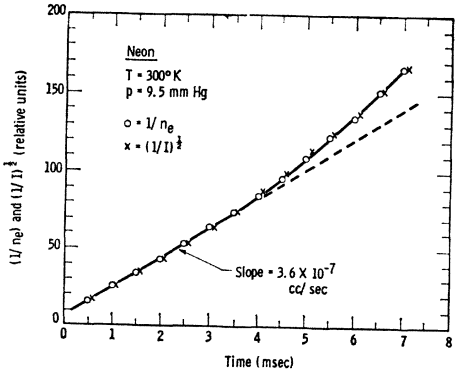

FIG. 6. Comparison of the electron density and the total intensity of visible radiation in a neon afterglow at 300°K. The $(\text{intensity})^{-1/2}$ curve is normalized to the $1/n_e$ curve at 2.5 msec in the afterglow.

In view of uncertainties in the viewing solid angle, stray reflections from walls, etc., the deduced values of α are considered significant only for their order of magnitude. From measurements in the afterglow when recombination is believed to predominate (e.g., Fig. 6), the quantum yields give values of $\alpha \sim 4 \times 10^{-7}$ for neon, and $\alpha \sim 10^{-6}$ for argon. (Similar measurements for helium are discussed in more detail in part II of this paper.) Thus, the absolute intensities of afterglow radiation are consistent with the α values deduced from fits of the electron density data to Eq. (4).

C. Effect of Molecular Ions

Having established the existence of the large volume recombination between electrons and positive ions, it still is necessary to determine the mechanism which leads to such efficient electron capture. As discussed in the introduction, the radiationless process of dissociative recombination, Eq. 2, has been suggested as the most likely reaction to explain our results. A distinguishing feature of this process is the fact that, although excited atoms are produced (substantiated by the observation, for example, that the afterglow radiation from neon consists of line spectra), the recombination requires the presence, initially, of molecular positive ions.

In order to test this idea, experiments were devised in which, in one case, molecular positive ions (Ar_2^+) and, in the second case, atomic ions (Ar^+) were expected to predominate during the afterglow.[19] It has been established that at moderate pressures, ~ 10 mm Hg, atomic ions of the noble gases are readily converted to molecular ions by a three-body reaction of the type[27]

$$Ar^+ + Ar + Ar \rightarrow Ar_2^+ + Ar. \quad (9)$$

At ~ 10 mm Hg pressure this reaction is expected to occur at a rate of the order of 10^4 sec^{-1} so that, on the millisecond time scale of our afterglow observations, even if the discharge contains a mixture of Ar^+ and Ar_2^+, the predominant afterglow ion rapidly becomes the molecular ion.

On the other hand, if one uses "dilute" mixtures of argon in helium gas (1 part in 10^3), ionization during the discharge will be predominantly of the Penning type,[24]

$$He^M + Ar \rightarrow He + Ar^+ + e, \quad (10)$$

where the superscript M indicates an atom in a metastable state. This reaction is possible because the metastable levels of the helium atom lie above the ionization limit of argon. At the low concentrations of argon atoms used, conversion to Ar_2^+ by reaction (9) or by the reaction,

$$Ar^+ + Ar + He \rightarrow Ar_2^+ + He, \quad (11)$$

should be too slow to produce significant argon molecu-

[27] The conversion rate for the analogous reaction in helium has been determined by A. V. Phelps and S. C. Brown, Phys. Rev. 86, 102 (1952).

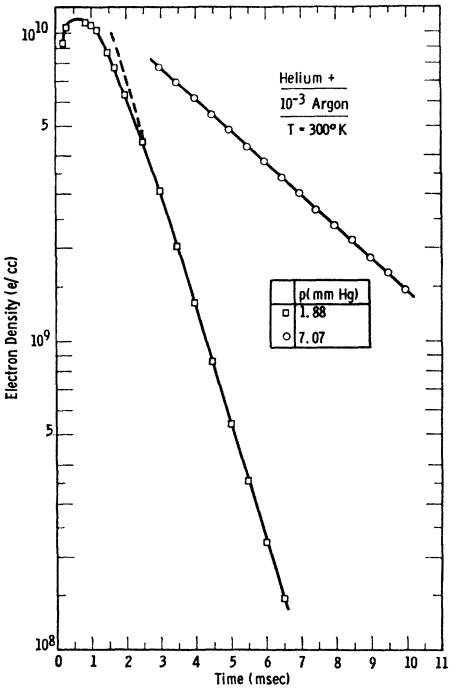

FIG. 7. Variation of the electron density during the afterglow in a helium-argon mixture at 300°K. The initial rise in the 1.88 mm Hg curve is the result of ionization of argon atoms by helium metastable atoms.

lar ion concentrations during the afterglow measuring period.[28]

Measurements of the decay of electron density have been carried out for the two cases described above.[19] In pure argon at 14 mm Hg pressure the observed electron decay is as shown in Fig. 3(b). The electron density decay obeys the recombination law (Eq. 4) over a range of approximately 30:1. The recombination coefficient, $\alpha=6\times10^{-7}$ cc/sec, obtained from correction[20] of the slope of the curve is in fair agreement with earlier work.[7] In view of the improved high vacuum system techniques used in the present experiment, it can be shown that no significant impurities were added to the argon samples[11] as a result of our gas-handling procedures. In addition, determinations of the absolute afterglow radiation intensity give a value of α consistent with that determined from the $1/n_e$ vs t curve.

In the case of helium-argon mixtures, in which Ar^+ ions are expected to predominate, a series of measurements have been carried out over the pressure range 1.7–7.1 mm Hg (the helium atom : argon atom ratio was 1000:1.15). The results of the measurements at two pressures are shown in Fig. 7, in which the electron density is plotted on a logarithmic and the time on a linear scale. It will be seen that the final decay is exponential in character and that the decay time constant increases linearly with pressure. Both of these characteristics are consistent with diffusion loss of electrons in the fundamental mode. The initial increase in electron density for the $p=1.88$ mm Hg curve is the result of ionization produced by metastable helium atoms,[24] Eq. (10).

From the final decay constant, T_1, the ambipolar diffusion coefficient of the Ar^+ ions and electrons in helium can be determined from the relation, $D_a=\Lambda_1^2/T_1$. The values deduced from the electron decay curves are shown in Fig. 8. It will be seen that, over the entire range, the pressure dependence appropriate to diffusion loss is verified. In addition, the value of the positive ion mobility, $\mu_+=21.5$ cm²/V-sec (at 300°K and a gas density of 2.69×10^{19} at./cc) deduced from the D_a measurements lies within 2% of the ion mobility vs mass number curve for helium[29] at the mass No.=40 position, thus supporting the assumption that the ion under study is Ar^+ not Ar_2^+.

In all cases, the electron-density decay curves (see Fig. 7) show no evidence of significant recombination loss (Eq. 4) at electron densities equal to or greater than the values at which recombination was dominant in pure argon [Fig. 3(b)]. From an analysis of the uncertainties in the experimental data of Fig. 7, we can set an upper bound to the recombination loss that might be present. It is found that α must be at least 1000 times smaller in the He-Ar mixture studies (Ar^+ ions) than in the pure argon measurements (Ar_2^+ ions).

The experimental evidence thus supports the hypothesis that in the helium-argon mixture studies we are predominantly observing the behavior of Ar^+ ions and electrons during the afterglow. Under these conditions only ionization of argon atoms by helium metastable atoms and ambipolar diffusion loss of electrons and ions are observed. Analysis of the data indicates that, when molecular ions are not present, the recombination loss of

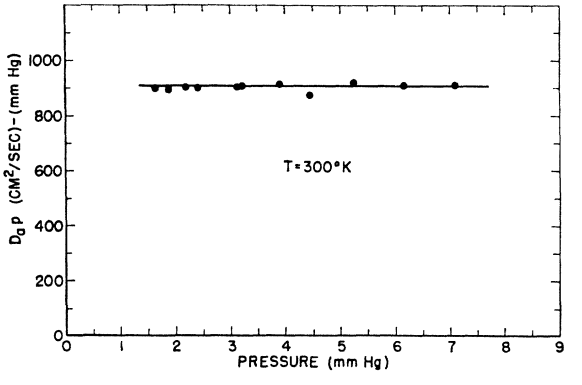

FIG. 8. Ambipolar diffusion coefficient of Ar^+ ions and electrons in helium at 300°K.

[28] In this work, we have neglected possible effects of $(HeAr)^+$ formation by the reaction, $Ar^+ + 2\,He \rightarrow (HeAr)^+ + He$; see, for example, M. Pahl and U. Weimer, Z. Naturforsch. **12a**, 926 (1957). The results of the experiment suggest that, if it is formed, $(HeAr)^+$ exhibits a very small recombination coefficient.

[29] A. F. Pearce, Proc. Roy. Soc. (London) **A155**, 490 (1936) and K. Hoselitz, *ibid.* **A177**, 200 (1941). A curve of mobility vs mass number is given in Fig. 8 of reference 18.

electrons is very small. Studies in neon-argon (1000:1) mixtures yield similar results, in that the electron density decay curves are accurately exponential in character, and thus are not at all consistent with the recombination decay curves, Eq. 4, observed in pure argon.

V. SUMMARY AND DISCUSSION

The present paper has presented experimental evidence that electron-ion recombination is an important electron removal process in ionized noble gases such as neon and argon. It has been shown that the decay of electron density with time during the afterglow following a discharge follows a volume recombination law, and that this decay is accompanied by a persistent emission of radiation from the volume of the ionized gas. If this radiation is attributed to the formation of excited atoms during the recombination process, then the absolute intensity of the afterglow radiation is consistent with the large recombination coefficients, $10^{-7}<\alpha<10^{-6}$ cc/sec, deduced from the measured electron-density decay curves. It is also shown that the afterglow radiation can be decreased by momentarily increasing the electron energy—consistent with the expectation that the rate of electron-ion recombination decreases with increasing electron energy.

Finally, the mechanism of the recombination process is investigated by comparing the electron decay curves under conditions in which first molecular ions and then atomic ions are expected to predominate during the afterglow. If dissociative recombination, Eq. 2, provides the efficient capture mechanism required to explain the large α values, it can only take place when molecular ions are present. It is shown that, under conditions when Ar_2^+ ions predominate, a large recombination loss of electrons is observed, while when Ar^+ ions are expected to predominate, only ambipolar diffusion loss of electrons and ions can be detected.

A second, more conclusive proof of the hypothesis that dissociative recombination is the process responsible for the large α values observed experimentally would be provided by detection of the kinetic energy of the dissociating atoms produced by the recombination event.[30] In part II of this paper we present the detailed results of experiments designed to detect the dissociation kinetic energy of the atoms produced during recombination in helium afterglows.

The author wishes to express his gratitude to T. Holstein for important contributions and stimulating discussions during the course of these experiments.

[30] M. A. Biondi, Phys. Rev. **93**, 650A (1954), W. A. Rogers and M. A. Biondi, Bull. Am. Phys. Soc. **2**, 87 (1957).

PHYSICAL REVIEW VOLUME 129, NUMBER 3 1 FEBRUARY 1963

Nuclear Quadrupole Interaction of Sb^{121} and Sb^{123} in Antimony Metal*

R. R. HEWITT AND B. F. WILLIAMS†
Department of Physics, University of California, Riverside California,
(Received 20 August 1962)

The five nuclear quadrupole resonances of Sb^{121} and Sb^{123} have been measured at 4.2°K giving the quadrupole couplings $eqQ=76.867\pm0.001$ and 97.999 ± 0.001 Mc/sec, respectively. The temperature dependence of the interaction has been measured from 2 to 480°K. Both isotopes have the same temperature dependence of $(1/\nu)(d\nu/dT)\approx2.4\times10^{-4}$ °K^{-1}. The ionic field gradient provides about 10% of this measured quadrupole coupling.

I. THE NUCLEAR ELECTROSTATIC INTERACTION WITH ITS ENVIRONMENT

THE general electrostatic interaction between a nucleus and those charge distributions external to that nucleus is

$$H=\int_{\tau_e}\int_{\tau_n}(\rho_n\rho_e/r_{en}-r_{en})d\tau_n d\tau_e \qquad (1)$$

where ρ_n is the charge density within the nucleus and ρ_e is the charge density external to the volume of the nucleus. This interaction may be written[1] as an expansion with respect to the charge centroid of the nucleus

$$H_k=\frac{4\pi}{2k+1}\sum_{q=-k}^{k}\int_{\tau_n}\rho_n r_n{}^k Y_q{}^{(k)}(\cos\theta_n,\varphi_n)d\tau_n \cdot\int_{\tau_e}\rho_e r_e{}^{-(k+1)}Y_{-q}{}^{(k)}(\cos\theta_e,\varphi_e)d\tau_e, \qquad (2)$$

where $Y_q{}^{(k)}$ are normalized tesseral harmonics and the dot indicates a tensor scalar product of degree k. The $k=0$ term is independent of orientation and not of direct

* Work supported in part by the National Science Foundation and the Research Corporation.
† National Science Foundation Cooperative Graduate Fellow.

[1] N. F. Ramsey, *Molecular Beams* (Clarendon Press, Oxford 1956).